

Phase-resolved spectroscopy and photometry of the eclipsing polar EP Draconis (=H1907+690)

A. D. SCHWOPE* and S. MENGEL, Potsdam-Babelsberg, Germany

Astrophysikalisches Institut Potsdam

Received 1996 November 5; accepted

We present phase-resolved optical spectroscopy and CCD photometry of the faint eclipsing polar EP Dra (H1907+690). A revised ephemeris is derived which connects all 32000 binary cycles since its discovery by Remillard et al. (1991). We found no difference between spin and orbital periods of the white dwarf. Changes in the light curve morphology are attributed to a different beaming behaviour which might change on timescales as short as one or several orbital periods. Optical light curve modelling was used to estimate the co-latitude of the accretion spot, which must be larger than 40° . We have detected Zeeman absorption lines of $H\alpha$ originating in an accretion halo in a field of 16 MG. The low-resolution spectra reveal no indication of resolved cyclotron harmonics, which is also suggestive of a relatively low field strength in the accretion region. The Balmer emission lines contain significant contributions from the UV-illuminated hemisphere of the companion star, whereas the HeII $\lambda 4686$ emission originates predominantly from the accretion stream. The emission lines have a multi-component structure and we could single out a narrow emission line in the $H\beta$ and $H\gamma$ lines. Its radial velocity amplitude suggests a low mass for the white dwarf, if the lines are interpreted as being of reprocessed origin from the whole illuminated hemisphere of the companion star.

Key words: Accretion – cataclysmic variables – AM Herculis binaries – stars: EP Dra – stars: eclipsing – stars: magnetic fields

AAA subject classification: 116; 117; 119

1. Introduction

EP Draconis belongs to the rare species of eclipsing AM Herculis binaries (‘polars’), of which less than ten are known to date. Discovered as optical counterpart of the HEAO-1 source 1H 1903+689 by Remillard et al. (1991, henceforth Rea91, who referred to it as H1907+690 because of a mismatch of the true position with the HEAO-1 error box), it attracted only little attention, mainly due to its faintness at optical wavelengths, $V \simeq 18^m$, and its short orbital period, $P_{\text{orb}} = 104.6$ min. The combination of both inhibited to collect detailed observational data with high phase resolution. Only one follow-up observation with the PSPC (position sensitive proportional counter) onboard ROSAT is reported by Schlegel and Mukai (1995). These latter observations showed the characteristic two-component spectrum of polars, consisting of a soft blackbody (10–15 eV) and a hard bremsstrahlung component. The eclipse was not clearly resolved at X-ray wavelengths, again due to the faintness of the system, i.e. low count rate, and a possible accumulated phase uncertainty at the time of the ROSAT observation. Hence, an accurate orbital period is necessary in order to reach an unambiguous interpretation of the X-ray data.

Eclipsing polars potentially offer good diagnostic opportunities for studies of the accretion geometry (and changes therein) and for studies of the stellar components of the system. We, therefore, have undertaken some efforts to improve our understanding of this system in particular and with it of the polars in general. Information about e.g. spin-orbit coupling, masses of the stars, magnetic field strength of the white dwarf, origin of line emission, which are of importance for the class as a whole, can be drawn only from studies of individuals and will be addressed in this paper.

The photometric observations of EP Dra served also as a test case for the capabilities of the renovated 70cm-telescope at the Astrophysical Institute Potsdam, which is located between the capitals of Berlin and Potsdam, hence, under a ‘beautifully’ illuminated sky.

*Visiting Astronomer, German-Spanish Astronomical Center, Calar Alto, operated by the Max-Planck-Institute für Astronomie jointly with the Spanish National Commission for Astronomy.

We describe our observations in Sect. 2, present the analysis of the light curves and the low-resolution spectra in Sects. 3 to 5 and close the paper with a short discussion of the main results in Sect. 6.

2. Observations of EP Dra

2.1. Low-resolution optical spectroscopy

EP Dra was observed with the 3.5m-telescope and Cassegrain double-beam spectrograph (TWIN) at Calar Alto, Spain, during two nights in August 1992 for each one orbital cycle. The exact dates of the observations are given in Table 1 together with information about the spectral and time resolution achieved. Inside the TWIN the beam is split by a dichroic at $\sim 5500 \text{ \AA}$ and fed into two separate spectrographs. These were equipped with low-resolution gratings and large-format CCDs (RCA $15\mu\text{m}$ at the blue arm, GEC $22.5\mu\text{m}$ at the red arm, RCA binned by 2 in spatial direction). We thus were able to cover the whole optical range at fairly good resolution with one shot. One drawback of the TWIN at that time was the relative long time needed for read-out and data storage, which resulted in an overhead of 2.5 min between successive exposures. This impacts strongly the phase-resolution of this 105 min binary or alternatively the signal-to-noise ratio achievable in individual spectra. In order to maximize the observing efficiency we used two different approaches in the two nights. In the first night we obtained *stepped* spectra where the object is jumped along the spectrograph slit while exposing (we collected spectral information at 10 positions in a 6300sec exposure), in the second night we obtained *trailed* spectrograms with the object trailing along the slit while exposing. We exposed for 7200sec with a trailing rate of $25''/\text{h}$, which resulted in phase resolutions as given in Tab. 1.

Table 1. Spectroscopic observations of EP Dra

date Y/M/D	time [UT]	D^{-1} $\text{\AA}/\text{mm}$	spectral range $\Delta\lambda$ \AA	spectral resol. FWHM \AA	spectra number	time/spect. sec	phase resol.
92/08/19	21:10 – 22:55	144	3330 – 5510	6	10	630	0.1
92/08/19	21:10 – 22:55	160	5590 – 9700	7–8	10	630	0.1
92/08/21	19:57 – 21:57	144	3330 – 5510	6	46	156	0.025
92/08/21	19:57 – 21:57	160	5590 – 9700	7–8	61	118	0.019

The observations were performed under good weather conditions with medium seeing of about $2''$. Observations of EP Dra were accompanied by taking bias-, dark- and flatfield frames. Helium-Argon arc line spectra were obtained each before and after the trailed and stepped spectra were taken. We observed a number of spectrophotometric standard stars during the observation run, which were used in order to flux-calibrate the spectra of EP Dra. They also provided background light sources suitable for determining the atmospheric absorption (O_2 , H_2O) in the near infrared.

The long exposure time used prevented a complete subtraction of the night sky lines, in particular in the red trailed spectrum. Neither linear nor high-order polynomial interpolation of the sky intensity above and below the region of the CCD exposed to EP Dra succeeded in a complete removal of the intense sky lines. This turned out to be due to our imperfect knowledge of the flatfield and reduced the usefulness of the red spectra longward of $\sim 7500 \text{ \AA}$. Another influence on the trailed spectra comes from slit losses due to imperfect guiding during the last third of the exposure caused by problems with the δ -encoder of the telescope. This influences mainly observations of EP Dra during the faint part of its orbital cycle and thus has no major impact on the analysis.

With the given setup of the grating angles we were left with a short uncovered wavelength interval between the blue and red spectra.

2.2. Differential photometry

Differential photometry of EP Dra was obtained during several nights in May and November 1995 with the 70cm reflector of the Astrophysical Institute Potsdam. The telescope was equipped with a large-format Tek-CCD with low read noise. All exposures of EP Dra were taken through a broad-band Johnson V-filter. These measurements were influenced by some transparency variations through clouds. The counts of EP Dra, which were measured through software-generated apertures, were, therefore, reduced to those of nearby field stars in the $8 \times 8 \text{ arcmin}^2$ field-of-view. In one of the nights a field with photometric standard stars was observed. We could thus derive a

crude photometric calibration with an uncertainty of about 0.3 mag. Some more details of the observations are given in Tab. 2.

Table 2. Photometric observations of EP Dra

date Y/M/D	time [UT]	filter	exposures	integration time sec
95/05/04	23:55 – 0:43	V	9	240
95/11/20	2:27 – 4:24	V	35	180
95/11/21	16:53 – 21:10	V	107	120
95/11/25	18:25 – 21:57	V	67	150
95/11/26	19:24 – 23:18	V	52	150

3. Light curves and eclipse ephemeris

In Fig. 1 we show the light curves of EP Dra as derived from the trailed spectrogram in the red arm of the TWIN and from our CCD photometry in comparison with the V-band light curve of Rea91. The light curve derived from the trailed spectrogram was computed by averaging over the wavelength interval 5650–5740Å and thus roughly corresponds to the standard V-band. At all occasions EP Dra displayed a similar light curve, which is characterized by two intensity peaks at start and end of the bright phase and the eclipse due to transit of the secondary star inbetween. The average faint-phase brightness in 1992 and 1995 was $V \simeq 18^m$, maximum brightness in the peaks was $V \simeq 17^m$.

We have measured the times of mid-eclipse in all our photometric and spectroscopic data (compiled in Tab. 3). An unweighted linear ephemeris to our new data combined with those measured by Rea91 gives an updated ephemeris for the time T_0 of mid-eclipse of

$$\text{HJD}(T_0) = 244\,7681.72918(6) + E \times 0.072656259(5), \quad (1)$$

where numbers in parenthesis indicate uncertainties in the last digits. Phases given in this paper refer to this updated ephemeris. The inclusion of a quadratic term in the regression did not improve the fit.

Table 3. Times of mid-eclipse of EP Dra from this work with their uncertainties

HJD +2400000	ΔT days	cycle	$O - C$ days
48854.4006	0.0010	16140	-0.0004
48856.3625	0.0006	16167	-0.0006
49842.5264	0.0010	29740	+0.0001
50047.4171	0.0003	32650	+0.0002

The phase difference between our updated ephemeris and that of Rea91 is only 0.003 phase units at the time of the ROSAT X-ray observations presented by Schlegel and Mukai (1995). Hence, if their X-ray light curve is shifted appropriately, it still displays the highest count rate around eclipse phase and a dip 0.15 phase units in advance (at phase 0.85). While the dip may be explained by the transient accretion stream, which is lifted out of the orbital plane, there is no explanation for the missing X-ray eclipse. According to the standard model for X-ray emission in polars, there must be a X-ray eclipse present when an optical eclipse is observed. It seems that problems with the X-ray data analysis might have corrupted the light curve.

The peaks in the optical light curves are caused by strong cyclotron beaming, hence, they contain information about the accretion geometry. With their estimate of the orbital inclination $i = 80^\circ$, and the observed length of the bright phase, Rea91 have also derived the probable location of the accretion spot, $\delta \sim 18^\circ$. Using this number at face value also for the inclination of the field line in the spot, the angle between the field in the spot and the line of sight varies between $\theta_{\min} = i - \delta = 62^\circ$ and $\theta_{\max} = 90^\circ$ only. This range, in particular the rate of change of θ with phase, appears very small and is likely to be unable to produce the observed sharp intensity peaks. We have

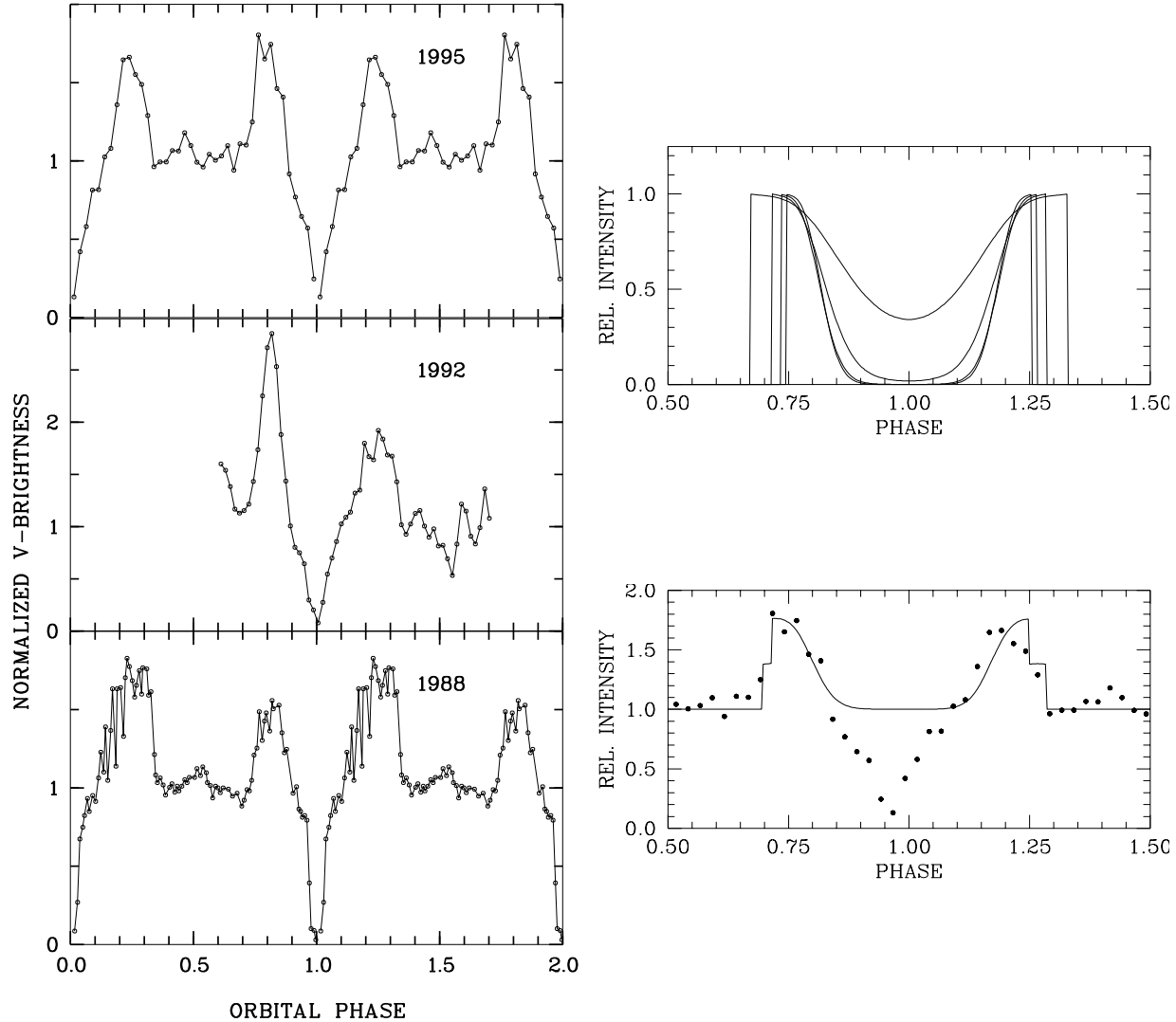


Fig. 1a) (left). Optical V-band light curves of EP Dra obtained at different occasions during recent years (*top*: AIP 70cm, *middle*: trailed spectrogram, *bottom*: data depicted from Rea91). All light curves were normalized to an approximate brightness level of 1 at phase $\phi_{\text{ecl}} = 0.5$. The data of 1995 and 1988 were phase folded, the light curve derived from the trailed spectrogram is shown in original time sequence.

b) (top right) Synthesized light curves of a cyclotron emitting accretion spot with zero extent. The orbital inclination was fixed at $i = 80^\circ$, the accretion spot colatitude was varied in steps of 20° between 20° (longest visibility) and 80° (shortest visibility). The phase convention defines minimum polar angle Θ as phase zero.

c) (bottom right) Synthetic light curve assuming two cyclotron spots compared with the 1995 observations.

therefore, undertaken some simple light-curve modelling using a tabulated cyclotron model from Wickramasinghe and Meggitt (1985) for $kT = 10$ keV, size parameter $\log \Lambda = 7$ and dimensionless frequency $\omega/\omega_c = 12$ (see next section for a motivation of these numbers). The visibility and radiation characteristic of a point-like accretion spot are calculated for a given aspect of the observer, orientation of the magnetic field and orbital phase.

Light curves resulting from this model are shown for fixed inclination $i = 80^\circ$ and different colatitude in Fig. 1b. Even this simple model yields constraints for the accretion geometry from a comparison of the observed and modelled width of the cyclotron peaks. The model light curves were calculated neglecting any extent of the accretion spot in horizontal or vertical direction, they are thus as sharp as theoretically possible. Any extent in either direction broadens the peaks. The observed peaks are certainly affected by some extent of the accretion region. We, therefore, use for the comparison the sharpest of the observed peaks, the first one in 1992, which then gives a lower limit to the colatitude δ . The peak width is measured as full width at 20% of maximum intensity measured with respect to the faint phase intensity. The width from the 1992 light curve is 0.127, the numbers for the synthesized light curves are given in Tab. 4. There is some systematic inconsistency introduced since the background light is time variable in the observed light curve, reaching a minimum around phase 0, while the background in the modelled light curve is constant. If we account for a variable background the true width of the observed peak might be as large as 0.155 phase units.

Table 4. Full width of intensity peaks at 20% level in synthesized light curves of Fig. 1b

colatitude	$\Delta\phi$	colatitude	$\Delta\phi$
20°	–	60°	0.109
30°	0.210	70°	0.105
40°	0.157	80°	0.099
50°	0.129		

The numbers given there show that the colatitude must be larger than $40^\circ - 50^\circ$. With $\delta = 50^\circ$ the visibility of the spot is only 0.55 compared to 0.64 as observed. This is clear evidence for an extended accretion region. Some constraints on the likely shape of the extended region comes from the fact, that the second peak in each of the observed light curves is broader than the first peak. This requires an elongated arc or ribbon which is better aligned with the terminator of the line of sight at start of the bright phase than at end. As a first approximation to the real situation we have modelled it using two spots (points) which may be regarded as endpoints of the arc. We again used $i = 80^\circ$, colatitudes $\delta_1 = 60^\circ$, $\delta_2 = 70^\circ$, a phase difference between both spots of 10° and a height of both regions of $0.005 R_{\text{wd}}$ (white dwarf radii). The resulting light curve is shown in comparison with our observed light curve of 1995 in Fig. 1c. Although not convincing in details (which is not surprising with the simple model assumptions), it reflects the main features of the observed light curve. It has the correct length of the bright phase, and the second peak is broader than the first.

At all occasions the light curves of EP Dra have the same length of the bright phase within 0.03 phase units. In addition, there is no significant shift of the bright phase with respect to eclipse center. Nevertheless, the length of the intensity peaks at start and end of the bright phase and their relative brightness may change drastically. Several implications can be drawn from this observation. Firstly, the spin-orbit coupling of the white dwarf is probably higher than 1×10^6 (inverse of fractional difference between the spin and the orbital periods). Secondly, the accretion arc has so far undergone no major migration towards different longitudes or latitudes. This is perhaps somewhat surprising because of its extreme position in stellar longitude, $\psi \simeq -17^\circ$. The center of the bright phase occurs after eclipse center, hence the magnetic axis points at the trailing side of the secondary star and thus resists the accretion torque which tries to turn the white dwarf to the leading side. Thirdly, although the accretion arc, which we regard as a region where accretion potentially may occur, seems to be a fixed structure, the actual distribution of matter (hot emission plasma) is highly variable, thus leading to different height and width of the cyclotron peaks.

A final comment in this section concerns the unpolarized radiation observed while the accreting pole is behind the white dwarf. It was regarded as of ambiguous nature by Rea91, being either thermal emission from an extended column above the white dwarf surface or reprocessed emission from the heated face of the secondary star. The key to answer this question lies in the Doppler tomograms shown below (Fig. 4) and the synthesized light curve of Fig. 1c. The former show line emission from the heated face of the companion star and the accretion stream and the latter show a significant decrease of the bright-phase intensity with respect to the model curve during the nominal bright phase outside the genuine eclipse. The intensity is there lower than during the nominal faint phase. Putting both things together, the likely nature of the unpolarized component is recombination radiation (line+continuum) from the accretion stream and the heated face of the secondary. Both are well observable outside the bright phase and start their eclipse much earlier than the accretion spot on the white dwarf. A rough estimate of the corresponding phases can be derived using the opening angle of the cone of the companion stars Roche lobe at the inner Lagrangian point L_1 , which is about 55° . The self-eclipse of the heated face of the secondary starts $90^\circ + 55^\circ$ prior to eclipse center, hence at $\phi_{\text{ecl}} \simeq 0.6$, the eclipse of the accretion stream starts with eclipse of L_1 , hence at $\phi_{\text{ecl}} \simeq 0.85$. These estimates show that large parts of the light curve may be affected by shadowing and obscuration of the very extended emission regions on the companion star and the accretion stream.

4. Signatures of the magnetic field

In Fig. 2 we show mean bright- and faint-phase spectra of EP Dra obtained in August 1992. They show the typical features of an AM Her star with strong H-Balmer and HeI, HeII emission lines superposed on a non-photospheric continuum. The continuum rises to the blue during the faint phase, it has maximum light in the red during the bright phase. On the assumption, that the excess light in the bright phase is only due to cyclotron radiation, a cyclotron spectrum can be computed by subtracting the mean faint-phase spectrum from the mean

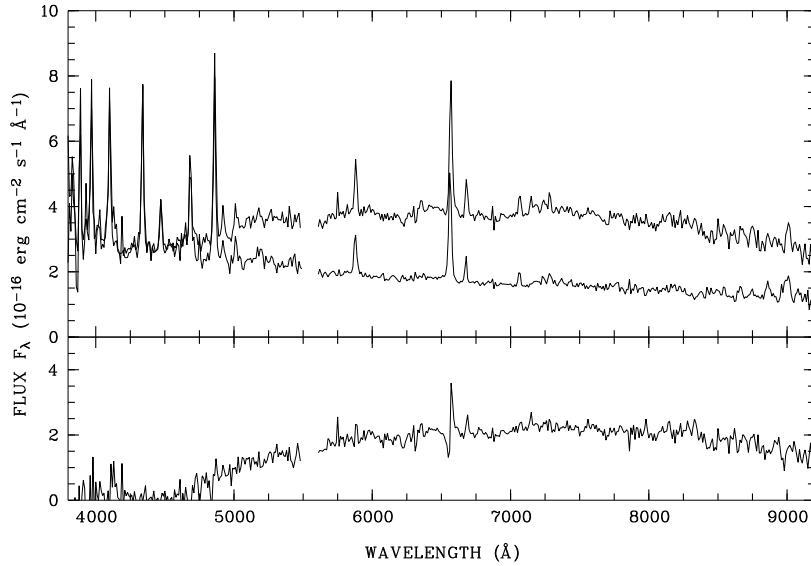


Fig. 2. (upper panel) Mean bright- and faint-phase spectra of EP Dra obtained in August 1992. (lower panel) Difference of the above spectra, regarded as cyclotron spectrum.

bright-phase spectrum. The difference spectrum is shown in the lower panel of Fig. 2, it is very red with peak intensity at $\sim 7000\text{\AA}$ and with no important contribution shortward of $\sim 5000\text{\AA}$.

The bright-phase spectrum shown in Fig. 2 was computed by averaging the stepped spectra before and after the eclipse centered on phases 0.790 and 0.277, respectively. A closer look on the trailed spectrum at around phase 0.8 is shown in Fig. 3. It displays two distinct flux minima more or less symmetric to the $H\alpha$ emission line. Such features have been found in several polars and were interpreted as Zeeman-split $H\alpha$ absorption lines in a cool halo surrounding the or intermixed with the hot emission plasma. This explains why the Zeeman lines are visible only against the bright cyclotron background and not during phases of low cyclotron brightness. We take the same view here and estimate the field strength in the halo to $B = 16$ MG. Below the observed spectrum we show the run of averaged Zeeman-split absorption components calculated assuming a Gaussian spread with $\sigma_B = 1$ MG around the central field of 16 MG. The absorption troughs of the σ^\pm -components are reflected well by this simple model, the π -component is filled in significantly by the strong emission line.

Three polars are known which show both, cool halo Zeeman absorption lines and hot plasma cyclotron emission lines (MR Ser, V834 Cen, and DP Leo, see Schwöpe (1995) for a complete compilation of measured field strengths in polars). In all three cases very similar values of the field strengths for both features were measured indicating the close coexistence of cool infalling matter and hot settling plasma and qualifying halo lines as tracers of the field strength in the accretion region. There is one possible counterexample, BL Hya, showing 12 MG halo lines (Schwöpe et al. 1995) and somewhat noisy 18 MG cyclotron lines (Ferrario et al. 1996). If we assume a field of 16 MG to be present in the cyclotron region too, the peak intensity of the observed cyclotron spectrum can be reflected with an isothermal 10 keV cyclotron model (see e.g. Schwöpe et al. 1995) with optical depth parameter $\log \Lambda \simeq 7$. At a field of 16 MG the spectral range between 5000\AA and 9000\AA corresponds to harmonic numbers 8.3 – 14.9 for a 10 keV plasma. In this regime significant harmonic overlap exists and we do not expect individual harmonics resolved, as observed. One might be tempted to identify some intensity humps in the bright-phase spectrum of Fig. 2 (e.g. at $\lambda\lambda 5900, 6500, 7300\text{\AA}$) with individual cyclotron harmonics, but this seems to us a combined effect of residual low-frequency fringing in the 2D-CCD spectrum, halo Zeeman absorption and a somewhat uncertain response function in the vicinity of the beam-splitting wavelength.

5. Emission lines and stellar masses

Our trailed spectrograms of EP Dra contain important information about the emission lines although the spectral resolution is rather low, 6\AA FWHM. The low spectral resolution is somewhat compensated by the good

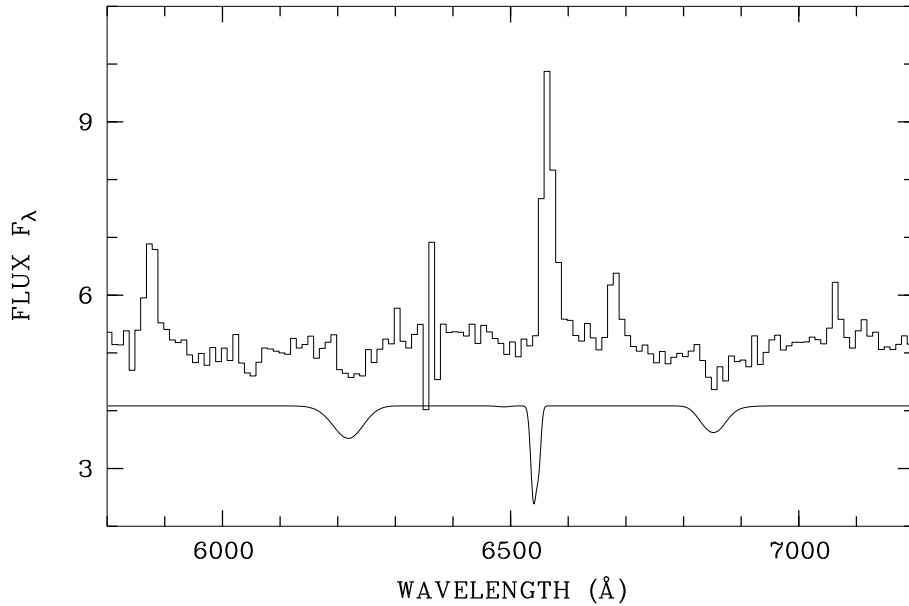


Fig. 3. Mean trailed bright-phase spectrum of EP Dra centered on phase 0.8 showing H α Zeeman absorption troughs. The model below the observed spectrum was calculated for a Gaussian distribution of the magnetic field with central field strength of 16 MG and spread σ_B of 1 MG.

phase resolution. As two examples we show in Fig. 4 the trailed spectra of the HeII $\lambda 4686$ and H β lines together with their Doppler images. The latter were computed by a filtered backprojection of the spectral lines. The spectra were continuum-subtracted for backprojection and representation in Fig. 4. Both lines have in common that they are bright before and after eclipse and that they show a flux depression between phases 0.35 and 0.5. The eclipse seems to be total for one or two phase bins, although definite statements cannot be drawn due to the low signal-to-noise ratio there. From phase 0.6 to 0.9 both lines show a pronounced motion from blue- to redshifts, between phases 0.05 and 0.35 in the opposite direction. This is naturally explained by emission from the accretion stream, which points away from us during eclipse and shortly thereafter. This stream component is rather broad, the measured width of ~ 15 Å FWHM corresponds to a velocity dispersion of ~ 900 km s $^{-1}$. The Balmer lines show in addition an unresolved line of much lower radial velocity amplitude which is most prominent at superior conjunction of the secondary star ($\phi_{\text{ecl}} \simeq 0.5$). It cannot be traced in the trailed spectrogram of the HeII line. This unresolved line is reminiscent of the narrow emission line of reprocessed origin from the secondary star, being so prominent in HU Aqr (Schwope et al. 1996). The Doppler image of H β supports this impression. If we compare the Doppler images of HeII $\lambda 4686$ and H β , it becomes clear, that the line emission in H β is much more concentrated on the secondary star (or the region of the inner Lagrangian point L_1) and that the HeII emission comes predominantly from the accretion stream. A sketch of possible locations of emission line regions, facilitating an understanding of the Doppler maps, is given also in Fig. 4.

Interestingly, the Doppler image of HeII $\lambda 4686$ is clearly different from that seen in HU Aqr, suggesting a much denser accretion curtain in EP Dra than in HU Aqr, which provides sufficient shielding of the companion star by absorbing ionizing EUV-photons.

We have measured the positions of the narrow emission lines of H β and H γ , whose trailed spectrograms look very similar, in the stepped spectra. This was done by fitting a double-Gaussian (narrow plus broad line) with fixed width of the narrow line. An unweighted sine fit to the measured positions in the phase interval 0.25–0.75, where both lines could be separated from each other, yielded a radial velocity amplitude of 210 ± 25 km/sec. This represents the center of line emission from some location on the illuminated hemisphere and can be used for a mass estimate of the white dwarf if some assumptions are fulfilled: 1) emission happens over that part of the Roche lobe which is geometrically accessible by radiation from the white dwarf, 2) ionizing radiation is reprocessed and re-emitted locally, 3) the secondary is a main-sequence star. We estimate the mass of the secondary star using the late-type star mass-radius relation given by Neece (1984) to be $M_2 = 0.133 M_\odot$. With (1) and (2) a geometrical reprocessing model (Beuermann and Thomas 1990) is applicable in order to transform center-of-light to center-of-mass radial velocities. This results in a mass ratio $Q = M_1/M_2 = 3.2 \pm 0.5$ and in a white dwarf mass of $M_1 = 0.43 \pm 0.07 M_\odot$. These results are only slightly dependent on the true value of the inclination, we used

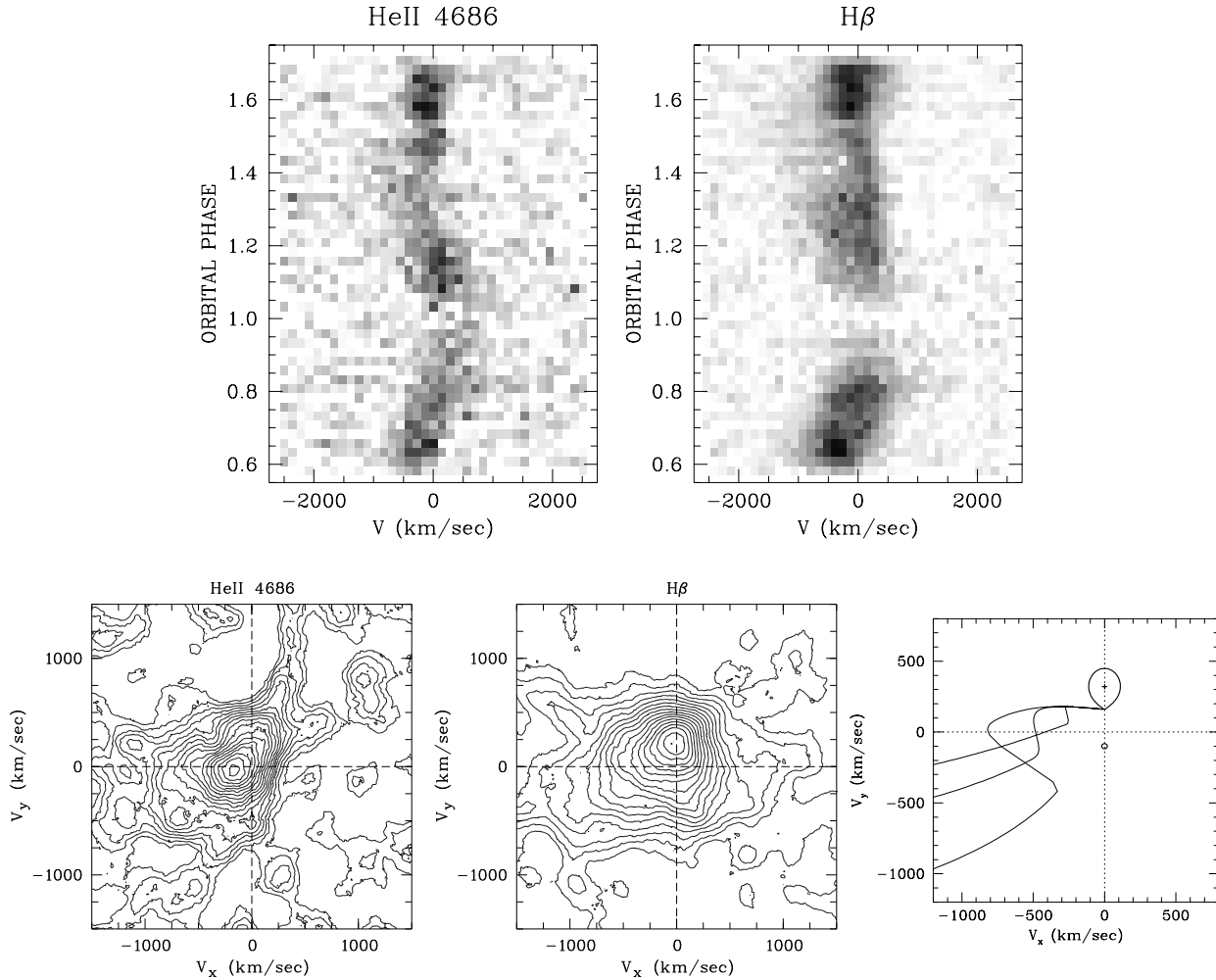


Fig. 4. Grey-scale representation of trailed, continuum-subtracted spectra of the HeII $\lambda 4686$ and H β lines of EP Dra. Phase runs along the ordinate from bottom to top, wavelength has been transformed to velocity using the rest wavelengths of the specified lines. In the lower panels the Doppler tomograms of the trailed spectra are shown computed by filtered backprojection.

(bottom right) Locations of the secondary star and the different parts of the accretion stream in the velocity-plane (v_x, v_y) for an assumed mass ratio of $Q = M_1/M_2 = 3.2$. Shown are the centers of mass of both stars (on the axis $v_x = 0$), the shape of the secondary star, a ballistic trajectory starting at the L_1 -point and that part of the stream which is guided by the magnetic field. We assumed three arbitrary loci of the coupling radius, chosen typically for AM Her stars in general and likely to occur in EP Dra also.

$i = 80^\circ$, but on the details of the illumination and the true mass-radius relation (which is rather uncertain). If the emission is concentrated towards the inner Lagrangian point L_1 , our value of M_1 would represent a lower limit only. However, taken the face values, the radial velocity amplitude gives evidence for a somewhat undermassive white dwarf.

6. Concluding remarks

We have presented the first phase-resolved spectroscopic and new photometric data of the eclipsing polar EP Dra. Using these we could improve on the accuracy of the eclipse ephemeris. We found no evidence for a quadratic term to be present in the ephemeris nor significant shifts of the bright phase with respect to eclipse center over a seven-year basis. Our models for the optical light curves reveal evidence for an extended accretion arc located at a stellar colatitude of about 60° – 70° . The X-ray light curve presented by Schlegel and Mukai (1995) remains ambiguous.

We have identified H α Zeeman absorption lines originating in an accretion halo at a field strength of 16 MG, which is a relatively low value compared to other AM Her stars. The red colour of the cyclotron spectrum is also suggestive of a relatively low field strength.

The trailed spectrograms of high- and low-ionization lines (e.g. HeII λ 4686, H β) are clearly different as well as the Doppler maps constructed from them. Balmer line emission is more concentrated on the heated face of the secondary and the region around L_1 , whereas stream emission is more prominent in HeII λ 4686. A possible explanation for the weakness of HeII λ 4686 emission from the secondary star is the presence of an accretion curtain providing effective shielding. If so, also the H-Balmer line is likely affected. Our radial velocity measurement of the secondary would probably be too low as well as our present estimate of the white-dwarfs mass, $M_1 = 0.43 \pm 0.07 M_\odot$.

Acknowledgements. We thank P. Notni for invaluable assistance at the AIP 70cm telescope and J.-U. Fischer, I. Lehmann and A. Schüller for patient observing during cold November nights in Potsdam. We acknowledge useful comments of the referee K. Beuermann. This work was supported by the DFG under grant Schw536/1-1 and the BMB+F under grant 50 OR 9403 5.

References

- Beuermann K., Thomas H.-C.: 1990, 1990, *Astron. Astrophys.* 230, 326
Ferrario L., Bailey J., Wickramasinghe D.: 1996, *Mon. Not. R. Astron. Soc.* 282, 218
Neece G.D.: 1984, *Astrophys. J.* 277, 738
Remillard R.A., Stroozas B.A., Tapia S., Silber A.: 1991, *Astrophys. J.* 379, 715 (Rea91)
Schlegel E.M., Mukai K.: 1995, *Mon. Not. R. Astron. Soc.* 274, 555
Schwope A.D.: 1995, *Rev. Mod. Astron.* 8, 125
Schwope A.D., Beuermann K.: 1989, *Astron. Astrophys.* 222, 132
Schwope A.D., Beuermann K., Jordan S.: 1995, *Astron. Astrophys.* 301, 447
Schwope A.D., Mantel K.-H., Horne K.: 1996, *Astron. Astrophys.*, in press
Wickramasinghe D.T., Meggitt S.M.A.: 1985, *Mon. Not. R. Astron. Soc.* 214, 605

Address of the authors:

Axel D. Schwope, Sabine Mengel
Astrophysikalisches Institut Potsdam
An der Sternwarte 16
D-14482 Potsdam
Germany
e-mail: ASchwope@aip.de

Figure 1: *(a, left)* Optical V-band light curves of EP Dra obtained at different occasions during recent years (*top*: AIP 70cm, *middle*: trailed spectrogram, *bottom*: data depicted from Rea91). All light curves were normalized to an approximate brightness level of 1 at phase $\phi_{\text{ecl}} = 0.5$. The data of 1995 and 1988 were phase folded, the light curve derived from the trailed spectrogram is shown in original time sequence. *(b, top right)* Synthesized light curves of a cyclotron emitting accretion spot with zero extent. The orbital inclination was fixed at $i = 80^\circ$, the accretion spot colatitude was varied in steps of 20° between 20° (longest visibility) and 80° (shortest visibility). The phase convention defines minimum polar angle Θ as phase zero. *(c, bottom right)* Synthetic light curve assuming two cyclotron spots compared with the 1995 observations.

Figure 2: *upper panel*: Mean bright- and faint-phase spectra of EP Dra obtained in August 1992. *lower panel*: Difference of the above spectra, regarded as cyclotron spectrum.

Figure 3: Mean trailed bright-phase spectrum of EP Dra centered on phase 0.8 showing H α Zeeman absorption troughs. The model below the observed spectrum was calculated for a Gaussian distribution of the magnetic field with central field strength of 16 MG and spread σ_B of 1 MG.

Figure 4: Grey-scale representation of trailed, continuum-subtracted spectra of the HeII $\lambda 4686$ and H β lines of EP Dra. Phase runs along the ordinate from bottom to top, wavelength has been transformed to velocity using the rest wavelengths of the specified lines. In the lower panels the Doppler tomograms of the trailed spectra are shown computed by filtered backprojection. *(bottom right)* Locations of the secondary star and the different parts of the accretion stream in the velocity-plane (v_x, v_y) for an assumed mass ratio of $Q = M_1/M_2 = 3.2$. Shown are the centers of mass of both stars (on the axis $v_x = 0$), the shape of the secondary star, a ballistic trajectory starting at the L_1 -point and that part of the stream which is guided by the magnetic field. We assumed three arbitrary loci of the coupling radius, chosen typically for AM Her stars in general and likely to occur in EP Dra also.